



Structural Investigations on Energy Storage Materials for Rechargeable Lithium Batteries

The rapid development of portable, computing and telecommunication devices has led to an increasing demand for high-energy-density rechargeable batteries. In particular, lithium batteries quickly became the most promising candidates to satisfy this demand and went forward to be applied in large-scale power systems, such as scooter and mobile car, etc. The principle for rechargeable lithium battery is illustrated in Fig. 1. A battery is composed of several electrochemical cells that are connected in series and/or in parallel to provide the required voltage and/or capacity. Each cell consists of a pair of positive and negative electrodes, separated by a non-aqueous electrolyte, in which Li^+ ions are transferred between these two electrodes. In practical application, capacity and stability of the electrode materials in repeated charge-discharge cycles are two major requirements. Both requirements are closely related to the structural

properties of electrodes.

Nowadays, there are many attractive materials used for cathode and anode in lithium batteries. For example, LiCoO_2 and LiNiO_2 of layered structure or LiMn_2O_4 of spinel structure are utilized as cathodes, and graphite carbon or lithium metal as anodes. The theoretical capacity of the cathode materials are 274 (LiCoO_2), 275 (LiNiO_2) and 148 (LiMn_2O_4) mAh/g, but for the anode materials they are 372 (graphite carbon) and 3830 (lithium metal) mAh/g, respectively. In this article, we report the recent progress in the development and characterization of electrode materials conducted by the groups led by Prof. Bing-Joe Hwang and Prof. Ru-Shi Liu, respectively.

LiCoO_2 was the first commercialized cathode material for lithium battery more than ten years ago. However, it has disadvantages in terms of cost and toxicity so that many efforts are focused on either reducing cobalt content via substitution by other transition metals, such as Ni, Cr, Mn, and Fe, or developing alternative materials. Spinel LiMn_2O_4 is currently one of the most favorable materials for large-scale lithium batteries because of its low cost, high rate capability, and environmental friendliness. Due to the disproportionation reaction in the electrolyte ($2\text{Mn}^{3+} \rightarrow \text{Mn}^{2+} + \text{Mn}^{4+}$) and the Jahn-Teller distortion at the end of discharge, LiMn_2O_4 exhibits capacity fading during the cycling. To solve these problems, surface modification and metal ion substitution have been applied on this material. It was found that the performance of the modified materials is strongly dependent on the variations of their short-range and long-range structures during the charge-discharge cycle.

LiMn_2O_4 based cathode materials assembled in

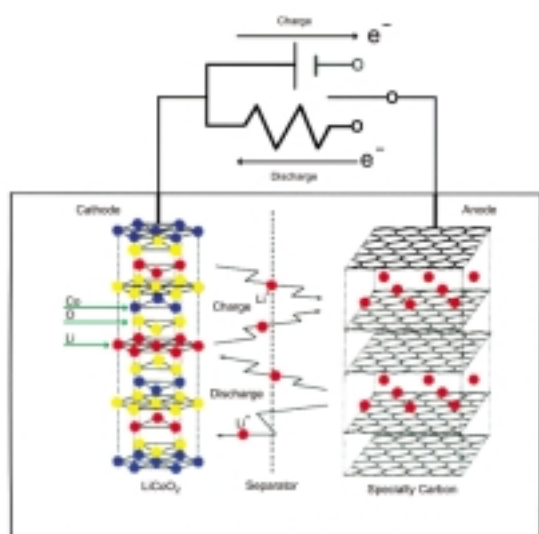


Fig. 1: Principle of rechargeable lithium battery.

a coin cell were investigated by means of *in-situ* X-ray absorption spectroscopy (XAS) and X-ray powder diffraction (XRD) by Hwang's group. These two complementary techniques provide structural information of short-range and long-range ordering, respectively. Moreover, the oxidation state of specific atom can be determined from the energy shift of absorption edge. These parameters are essential for understanding the intercalation mechanism and fading mechanism of the materials and hence improving their performance. The XRD and XAS measurements were carried out at the wiggler beamlines BL17A1 and BL17C1 of SRRC, respectively.

A $\text{LiAl}_{0.15}\text{Mn}_{1.85}\text{O}_4/\text{LiPF}_6+\text{EC}+\text{DEC}/\text{Li}$ cell was charged at 0.2 C-rate and discharged at 0.1 C-rate in the potential range from 3.3 to 4.3 V vs. Li/Li^+ . The discharge curve of $\text{Li}_x\text{Al}_{0.15}\text{Mn}_{1.85}\text{O}_4$ electrode, shown in Fig. 2, indicates that its specific capacity is about 110 mAh/g, slightly less than the theoretical capacity (125 mAh/g). The corresponding x values

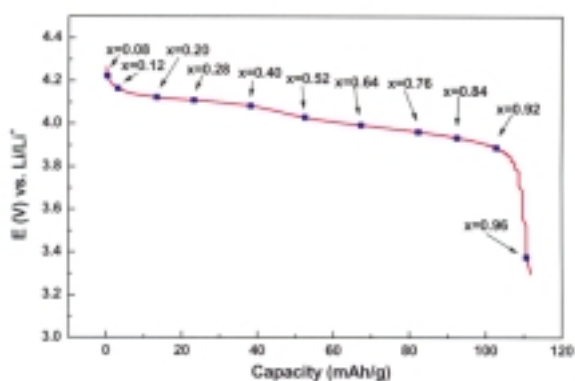


Fig. 2: Discharge curve of $\text{Li}_x\text{Al}_{0.15}\text{Mn}_{1.85}\text{O}_4$ cathode material in the potential range between 4.3 and 3.3 V at 0.1 C-rate.

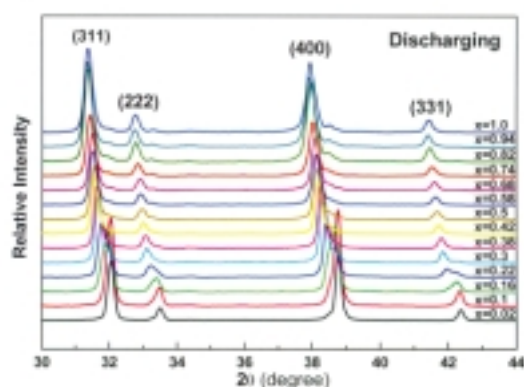


Fig. 3: XRD patterns of $\text{Li}_x\text{Al}_{0.15}\text{Mn}_{1.85}\text{O}_4$ cathode material at various x-values during discharge.

shown in Fig. 2 represent the amounts of lithium intercalated into the spinel structure during discharge. From the X-ray absorption near edge spectra (not shown here), it was found that the average valence of Mn reduced from 4 to 3.5 in the discharging process. Figs. 3 and 4 respectively display the XRD patterns of $\text{Li}_x\text{Al}_{0.15}\text{Mn}_{1.85}\text{O}_4$ electrode and the Fourier transformed k^3 -weighted EXAFS spectra at Mn K-edge at various x values during discharge. These results indicate that a phase transition from cubic phase I to cubic phase II occurs in the x region between 0.16 and 0.3 (Fig. 3) and the contribution of the second shell Mn-Mn interaction reduces gradually from the x value 0.08 to 0.52 (Fig. 4). Beyond the above region, the change in magnitude of radial distribution function becomes relatively small as the phase transition is nearly complete. Detailed EXAFS data analysis indicates that both the interatomic distance and Debye-Waller factor for the first three coordination shells, Mn-O(2), Mn-O(4) and Mn-Mn, become larger with an increase in the x value. Thus, the local structure of this material seems more disordered at discharged state than that at charged state. It was generally recognized that the phase transition is the main reason for capacity fading of LiMn_2O_4 . Accordingly, suppression of the occurrence of phase transition should enhance the structural stability and eliminate the capacity fading. In this aspect, substitution of a small portion of Mn^{3+} in LiMn_2O_4 by Al^{3+} results in significant improvement as compared with the pure LiMn_2O_4 compound.

Liu's group, on the other hand, put their efforts

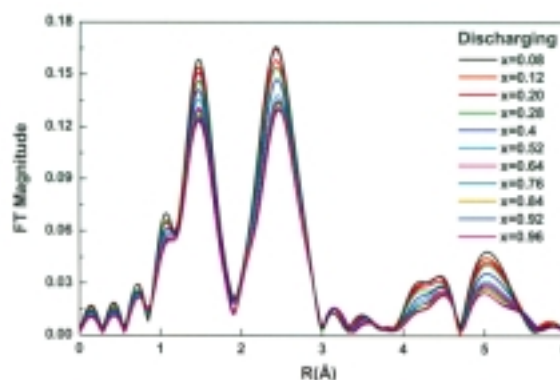


Fig. 4: Fourier transformed k^3 -weighted EXAFS spectra of $\text{Li}_x\text{Al}_{0.15}\text{Mn}_{1.85}\text{O}_4$ at Mn K-edge at various x values during discharge.



to explore a new anode material LiVMoO_6 . Normally, LiVMoO_6 is accepted as a cathode material due to its layered structure. However, Liu et al. used this material as an anode because of the difficulty to oxidize the high valence of V and Mo during charge. The LiVMoO_6 sample was synthesized via standard solid-state reaction using Li_2CO_3 , V_2O_5 and MoO_3 as the starting materials. LiVMoO_6 crystallizes to the brannerite (ThTi_2O_6) structure which consists of edge- and corner-sharing MO_6 ($M = \text{V}$ or Mo) octahedra. The negative charges on the M_2O_6 sheets are compensated by additional cations (Li^+) which reside in the interlayer space.

X-ray absorption near edge structure (XANES) spectra of LiVMoO_6 and standard samples collected at the V and Mo K-edges are shown in Fig. 5. According to the chemical shift of the LiVMoO_6 spectra, the oxidation number of the vanadium is estimated to be around 4.5, but that of molybdenum ion is 6. Electrochemical characterization is performed using the coin-type cell, which was cycled using a Maccor automatic cycling/data recording system at a current density of 0.3 mA/cm^2 . When the cell was cycled between 3.00~0.01 V (Fig. 6), the potential rapidly drops to

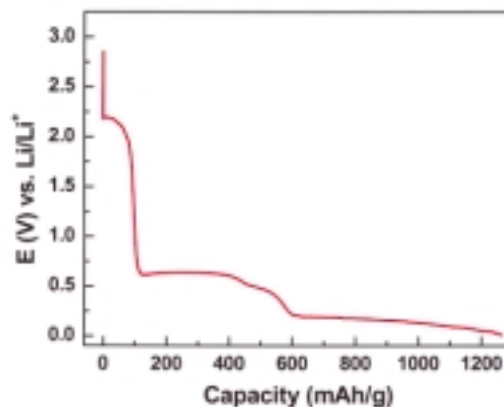


Fig. 6: Discharge curve of LiVMoO_6 anode material in the potential range between 3.00 and 0.01 V at a current density of 0.3 mA/cm^2 .

reach a plateau, and then continuously decreases down to 0.01 V. The amplitudes of three plateaus are approximate 2.1-2.0 V, 0.6-0.5 V and 0.2-0.01 V, respectively. The total discharge capacity, averaged over several test runs, is about 1250 mAh/g, which is much higher than that of the conventional graphite-type materials.

In summary, the Li-based battery research is relatively young, and as such is a source of aspirations as well as numerous exciting challenges. Through material design and synthesis we can expect significant improvements in the energy density. Although the efforts are highly multidisciplinary with strong roots in the fields of chemistry, physics and interfacial sciences, a better understanding of charging-discharging mechanisms of the cells, which can be achieved by *in-situ* X-ray absorption and diffraction studies, is of great importance to facilitate the design of new materials.

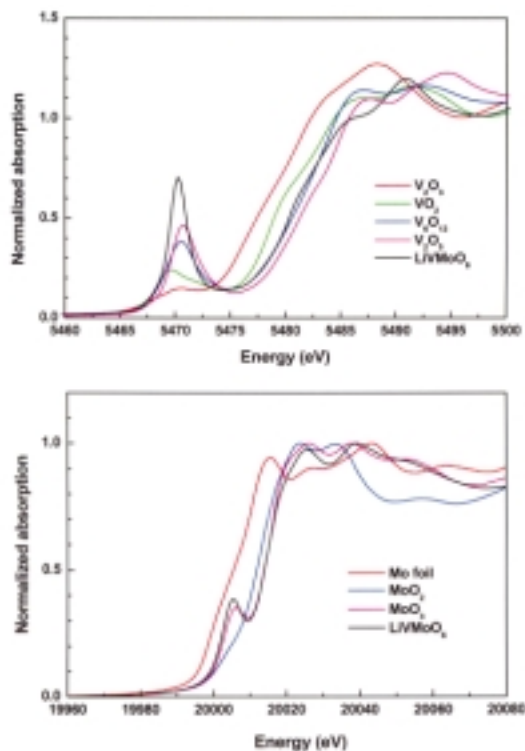


Fig. 5: XANES spectra of LiVMoO_6 in comparison with the standard samples at the V and Mo K-edges.

Beamlines:

17A1 Wiggler beamline

17C1 Wiggler beamline

SPring-8 BL12B2 beamline

Experimental Stations:

Powder diffraction end station

EXAFS end station

Authors:

B. J. Hwang

Department of Chemical Engineering, National Taiwan University of Science and Technology, Taipei, Taiwan

R. S. Liu

Department of Chemistry, National Taiwan University, Taipei, Taiwan

J. F. Lee, H. S. Sheu

Synchrotron Radiation Research Center, Hsinchu, Taiwan

Publications:

- B. J. Hwang, R. Santhanam, C. P. Huang, Y. W. Tsai, and J. F. Lee, *J. Electrochem. Soc.*, **149**, A694 (2002).
- B. J. Hwang, R. Santhanam, and S. G. Hu, *J. Power Sources*, **108**, 250 (2002).
- B. J. Hwang, Y. W. Tsai, G. T. K. Fey, and J. F. Lee, *J. Power Sources*, **97-98**, 551 (2001).
- C. H. Shen, R. Gundakaram, R. S. Liu, and H. S. Sheu, *J. Chem. Soc. Dalton Trans.*, 37 (2001).
- B. Ammundsen, J. Paulsen, I. Davidson, R. S. Liu, C. H. Shen, J. M. Chen, L. Y. Jang, and J. F. Lee, *J. Electrochem. Soc.*, **149**, A431 (2002).

Contact e-mail:

bjh@ch.ntust.edu.tw